Aust. J. Phys., 1992, **45**, 695–716

Group Travel Time of EM Waves with Frequencies near the Ion Cyclotron Frequency in the Two-ion Magnetosphere

Y. D. Hu and B. J. Fraser

Physics Department, University of Newcastle,
Newcastle, N.S.W. 2308, Australia.

Abstract

The oblique propagation of electromagnetic (EM) waves with frequencies below the equatorial proton cyclotron frequency is investigated for a two-ion magnetospheric plasma. Attention is focused on the wave group travel time along a geomagnetic field line from the equatorial wave source region to the ionosphere or the location where the wave is reflected. It is found that the coupling between left- and right-hand polarised waves occurring at a crossover frequency significantly modifies features of the frequency–time spectrum. Because of this modification, the spectral tone change of Pc 1 waves observed on the ground (e.g. Dowden 1966; Gendrin and Laurent 1979) is not caused solely by dispersion effects in a multi-component plasma. The method used in this paper to calculate the wave group travel time provides further understanding of wave propagation in the magnetosphere, and is important for the estimation of magnetospheric plasma parameters using Pc 1–2 ground records.

1. Introduction

In this paper we consider the group travel time for EM waves with frequencies near the ion cyclotron frequency in a multi-ion magnetospheric plasma. The ground signatures of these waves are Pc 1–2 geomagnetic pulsations (~0·1–5 Hz). The waves are generated in the magnetosphere over $L \sim 3$–9, through a resonant interaction of left-hand polarised ion cyclotron waves with energetic and anisotropic ions in the ring current, and then propagate away from their source regions, whereby some of the wave energy may propagate to the ground. Because the waves propagate through the magnetosphere, they have often been used as a diagnostic tool to obtain information on the properties of the magnetospheric plasma. One of the important diagnostic parameters is the wave travel time between the two hemispheres. In an inhomogeneous plasma, if temporal and spatial scales for the variations of the background plasma are much greater than the wave period and wavelength respectively, then the wave packets propagate at the wave group velocity in the plasma according to the WKB theory (e.g. Chen 1987). In this situation, the wave travel time is the wave group travel time. For structured Pc 1–2 waves, the wave travel time relates to the interhemispheric bounce period of wave packets. This bounce period has been employed to explain the fine structure observed in structured Pc 1–2 pulsation dynamic spectra (see Jacobs and Watanabe 1964; Obayashi 1965; Dowden 1965; Gendrin *et al.* 1971). Because the wave travel time depends on the wave dispersion characteristics in the magnetospheric thermal (or cold) plasma, and the L value of the wave propagation path, computation of the wave group travel time provides a connection between

0004-9506/92/050695$05.00

the observed wave spectral structure and the thermal plasma parameters and the wave path in the magnetosphere.

In early studies of the wave travel time, the plasma was considered to contain only electrons and protons (Obayashi 1965; Dowden and Emery 1965; Gendrin *et al.* 1971; Higuchi *et al.* 1972). Hence, the waves remained left-hand polarised when propagating in this single-ion magnetosphere, and the wave normal angle θ (the angle between $\boldsymbol{k}$ and $\boldsymbol{B}_{\mathrm{E}}$ where $\boldsymbol{k}$ is the wave vector and $\boldsymbol{B}_{\mathrm{E}}$ is background magnetic field) did not significantly influence the wave travel time in the magnetosphere (e.g. Dowden 1965). In this case, the waves are guided along the magnetic field, i.e. the angle between the group velocity direction and $\boldsymbol{B}_{\mathrm{E}}$ remains small during propagation. When the waves reach the top of the ionosphere, θ increases to 90° (Dowden 1965; Kitamura and Jacobs 1968). It is believed that the waves are reflected in the region where θ reaches 90°. This reflection leads to the ion cyclotron wave packet bouncing between two hemispheres.

It has been recognised that wave dispersion properties are controlled by the concentration of thermal heavy ion species, such as He^+ (Young *et al.* 1981; Roux *et al.* 1982; Fraser 1982) and/or O^+ (Fraser and McPherron 1982; Inhester *et al.* 1984). In the presence of heavy ion species, there are modifications to the dispersion relation, which affect the computation of the wave group travel time:

(i) stop bands for left-hand polarised waves near ion cyclotron frequencies (Smith and Brice 1964; Mauk *et al.* 1981);
(ii) reflection of left-hand polarised waves at cutoff frequencies;
(iii) coupling between left- and right-hand polarised waves at crossover frequencies (Smith and Brice 1964; Gurnett *et al.* 1965);
(iv) reflection and transmission of right-hand polarised waves at multi-ion hybrid resonant frequencies (Rauch and Roux 1982; Perraut *et al.* 1984).

When wave propagation is strictly parallel, the crossover of wave polarisation will not occur, and the waves remain left-hand polarised (i.e. ion cyclotron mode). If wave frequencies are below the cyclotron frequency of the heaviest ion species, these waves can propagate in the magnetosphere in a way similar to the propagation in an e^-–H^+ plasma except that the ion cyclotron frequency is lower. However, if the wave frequencies are above the cyclotron frequency of the heaviest ion species, these waves will be reflected in a region where the wave frequency matches local cutoff frequencies induced by other ion species. Higuchi (1985) discussed the wave group travel time for the parallel propagation of ion cyclotron waves. He only considered the waves with frequencies below the cyclotron frequency of the heaviest ion species. Dowden (1966) and Fraser (1972) also studied the wave group travel time for ion cyclotron wave parallel propagation. In their studies, the complete wave frequency range $F < F_{\mathrm{c}}(H^+)$ was included. In order to avoid the difficulty caused by the cutoff frequencies, these authors assumed that the ions heavier than H^+ were confined within a narrow equatorial region (e.g. latitude ±10°), so that the wave frequencies considered would never match the cutoff frequencies. This assumption does not represent the real spatial distribution of heavy ions. However, because the greatest contribution to group travel time calculations occurs in the equatorial region where the waves have minimum group velocity, heavy ions at latitude above 10° were considered

unimportant in these papers for the travel time calculations. This assumption is robust for all properties other than wave cutoff and, as discussed in Section 3, the assumption probably breaks down in this regard when the heavy ion concentration is larger than 1%. When $\theta \neq 0$, i.e. oblique propagation, all four modifications mentioned above will affect the wave group travel time. Particularly, it can be expected that the presence of the crossover of wave polarisation will couple some energy from the ion cyclotron mode into the right-hand polarised magnetosonic mode, thus allowing some propagation through the cutoff of left-hand polarised waves. Also, multi-ion hybrid resonances may appear.

In diagnostics, computation of the wave group travel time in an e^-–H^+ plasma can be used only for the rising tone fine structure of Pc 1–2. However, the Pc 1–2 spectra often show complicated structures (Tepley 1966; Dowden 1966; Fraser 1972; Fraser-Smith 1977). The heavy ion modification to the wave group travel time was used to explain the change of tones in observed spectra (e.g. Dowden 1966; Fraser 1972; Gendrin and Laurent 1979). Using the parallel dispersion relation for the ion cyclotron waves in an e^-–He^+–H^+ plasma, Fraser (1972) developed a method that determines the propagation path of 'nose' pulsations, and the proton and helium concentrations at the top of the path in the equatorial region. Because of the importance of the wave group travel time in the Pc 1–2 spectra, further study of the computation of this parameter will lead to increased understanding of the dynamics of Pc 1–2 in the magnetosphere, and to a more reliable and accurate estimation of wave propagation paths and plasma parameters.

The purpose of this paper is to develop a method to calculate the wave group travel time in an e^-–He^+–H^+ plasma taking account of oblique propagation. Consideration of mode coupling between left- and right-hand polarised waves is included. It will be shown that the characteristics of oblique propagation are significantly different from those of parallel propagation.

2. Computation of the Wave Travel Time

Consider a wave packet propagating in the magnetosphere. The group travel time is

$$T_g = \int |\boldsymbol{V}_g|^{-1} \, ds , \tag{1}$$

where $\boldsymbol{V}_g$ is the wave group velocity, and ds is the distance element. The integral is along the wave path. Both $\boldsymbol{V}_g$ and the wave path in the magnetosphere depend on the wave dispersion relation and wave normal angle θ. Therefore, it is necessary to study the local wave dispersion characteristics (e.g. local group velocity) and the variation of the wave parameters (e.g. wave normal angle) in the magnetosphere before we calculate T_g.

(2a) Dispersion Relation and Group Velocity

Although the plasma in the magnetosphere is in the thermal energy range (0·1–10 eV), the ion temperature does not change topological properties of the dispersion relation (Hu 1991) and only leads to slight modification of the values of the phase and group velocities (e.g. Higuchi and Jacobs 1970). In the following study, we consider mainly effects caused by the change in topology of the wave dispersion relation in the presence of heavy ion species, and therefore use a cold

plasma approach to describe the magnetospheric bulk plasma. This approach has already been widely used in studies of electromagnetic waves with frequencies near the ion cyclotron frequencies in magnetospheric multi-component plasmas (e.g. Dowden 1966; Fraser 1972; Rauch and Roux 1982).

We consider here a magnetosphere with two ion species (H^+ and He^+), because the two-ion plasma is sufficient to illustrate the basic pattern of the modifications on the wave dispersion relation introduced by multiple ion species. Physical properties obtained from the two-ion plasma can, in principle, also be applied to other plasmas with more than two ion species (e.g. an e^-–O^+–He^+–H^+ plasma).

When plasma waves propagate in a cold, infinite, homogeneous, and collisionless plasma within a uniform magnetic field in the z direction, i.e. $\boldsymbol{B}_E = B_E \boldsymbol{e}_z$, the wave dispersion relation is given by (e.g. Stix 1962)

$$An^4 - Bn^2 + C = 0, \qquad A = S\sin^2\theta + P\cos^2\theta,$$

$$B = RL\sin^2\theta + PS(1+\cos^2\theta),$$

$$C = PRL, \qquad S = (R+L)/2,$$

$$R = 1 - X_p(e)^2 X^{-1}[X - X_c(e)]^{-1} - \sum_{\substack{i=\text{ion}\\ \text{species}}} X_p(i)^2 X^{-1}[X + X_c(i)]^{-1},$$

$$L = 1 - X_p(e)^2 X^{-1}[X + X_c(e)]^{-1} - \sum_{\substack{i=\text{ion}\\ \text{species}}} X_p(i)^2 X^{-1}[X - X_c(i)]^{-1},$$

$$P = 1 - X_p(e)^2 X^{-2} - \sum_{\substack{i=\text{ion}\\ \text{species}}} X_p(i)^2 X^{-2}, \tag{2}$$

where n is the refractive index, X is the wave frequency normalised by the proton cyclotron frequency, and X_p (e or i) and X_c (e or i) are normalised electron or ion plasma and cyclotron frequencies respectively. The solution of this dispersion relation can be expressed as $n^2 = [B \pm (B^2 - 4AC)^{1/2}]/2A$. The wave polarisation is given by $\rho = (n^2 - S)/D$ where $D = (R - L)/2$. When $\rho > 0$, the wave has right-hand polarisation; when $\rho < 0$, the wave has left-hand polarisation; and when $\rho = 0$, the wave has linear polarisation.

For a plasma with H^+ and He^+ ions, there are three continuous curves in X–k ($k = |\boldsymbol{k}|$) space when $0 < \theta < 90°$ (Fig. 1). If a wave belongs to one of the curves at a spatial point, it will remain on the same dispersion curve when propagating in an inhomogeneous medium. These curves are named as (e.g. Rauch and Roux 1982; Fraser 1985):

Class 1—$0 < X < X_c(He^+)$, left-hand polarised;

Class 2—when $X_{cf}(He^+) < X < X_{cr}(He^+)$, left-hand polarised; when $X > X_{cr}(He^+)$, right-hand polarised;

Class 3—when $0 < X < X_{cr}(He^+)$, right-hand polarised; when $X_c(H^+) > X > X_{cr}(He^+)$, left-hand polarised;

where X_{cf} is a cutoff frequency given by the solution of $L = 0$ (i.e. the left-hand waves are cut off at this frequency), X_{cr} is a crossover frequency given by the solution of $R = L$. For the e^-–He^+–H^+ plasma, $X_{cf}(He^+) = [1 + 3N(He^+)/N(e)]/4$ and

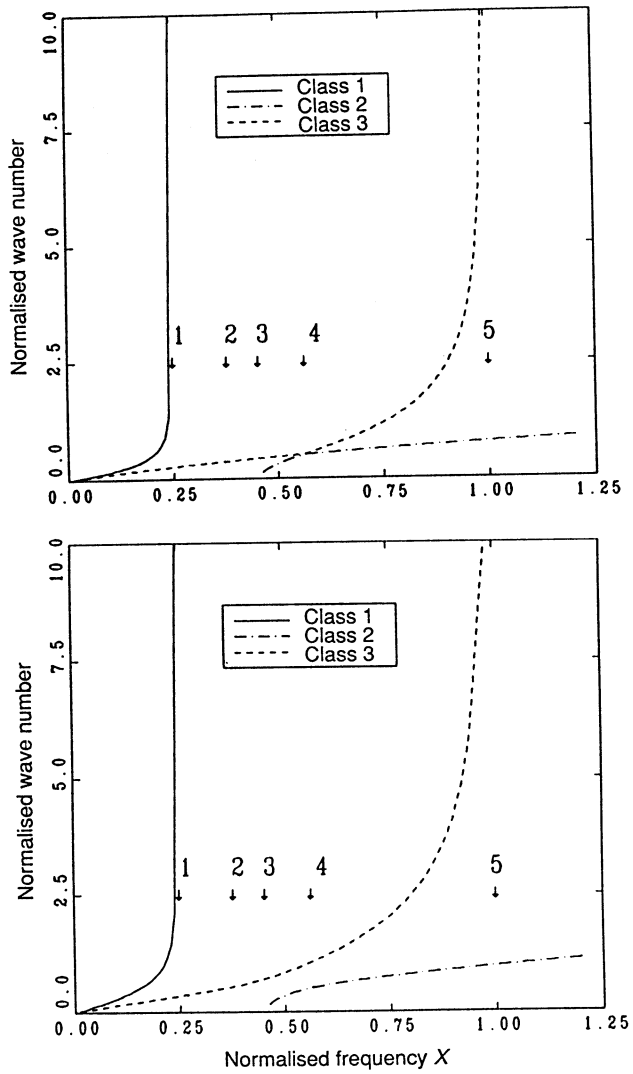

Fig. 1. Wave dispersion relation in an e^-–He^+–H^+ plasma with $N(He^+)/N(e) = 0{\cdot}27$. The top panel is for $\theta = 10°$ and the bottom panel for $\theta = 60°$. Arrows 1 to 5 indicate $X_c(He^+)$, X_{bi}, X_{cf}, X_{cr} and $X_c(H^+)$ respectively.

$X_{cr}(He^+) = [1 + 15N(He^+)/N(e)]^{1/2}/4$, where N is the particle number density. The presence of a heavy ion species introduces a coupling, for $\theta \neq 0$, between left- and right-hand polarised waves at a crossover frequency X_{cr}, where the waves become linearly polarised. When $\theta = 0$ at the crossover frequency, although the phase velocities for the left- and right-hand modes are the same, these modes remain decoupled since their group velocities are different (Leer *et al.* 1978). The stop band induced by the heavy ions for the left-hand polarised waves is between X_c(heavy ion species) and X_{cf}. When θ is close to 90°, the additional ion

species causes a hybrid resonance at a hybrid frequency X_{bi}. For the e^-–He^+–H^+ plasma, $X_{bi}(He^+) = \{[1 + 3N(He^+)/N(e)][1 + 3N(He^+)/4N(e)]^{-1}\}/4$.

As an example, we consider a plasma with $N(He^+)/N(e) \sim 0{\cdot}27$. The characteristic frequencies are $X_{bi} = 0{\cdot}378$, $X_{cf} = 0{\cdot}453$ and $X_{cr} = 0{\cdot}564$. Therefore, class 1 has $0 < X < 0{\cdot}25$, class 2 has $0{\cdot}453 < X$ (when $0{\cdot}453 < X < 0{\cdot}564$, left-hand polarised; and when $X > 0{\cdot}564$, right-hand polarised), and class 3 has $0 < X < 1$ (when $0 < X < 0{\cdot}564$, right-hand polarised; and when $0{\cdot}564 < X < 1$, left-hand polarised). These are shown in Fig. 1.

It is necessary to mention that the concentration of He^+ ions is assumed to be $N(He^+)/N(e) = 0{\cdot}27$ along the $L \sim 4{\cdot}6$ field line. It has been found that the typical value for He^+ concentration in the equatorial plasmapause region ($L \sim 4$–6) is between $0{\cdot}1$ and $0{\cdot}6$ (e.g. Geiss *et al.* 1978; Young *et al.* 1981; Balsiger *et al.* 1983). Furthermore, oblique wave propagation characteristics remain qualitatively the same if the heavy ion concentration is in the measured range ($\sim 0{\cdot}05$–$0{\cdot}6$). In this paper, attention is focused on the method used to calculate the wave group travel time and on the physical properties of the wave propagating obliquely in the two-ion plasma. It will be shown later that for a heavy ion concentration between $0{\cdot}1$ and $0{\cdot}6$, the ground-observed wave frequency–time relationship is determined by oblique propagation with mode coupling, rather than by parallel propagation. Since the choice of the value of the heavy ion concentration from the range $0{\cdot}1$–$0{\cdot}6$ does not qualitatively affect wave propagation properties, our assumed value is reasonable. However, when considering a specific wave event quantitatively, the choice of the He^+ concentration should be examined carefully.

Since the waves are generated by the ion cyclotron interaction, only left-hand polarised modes in wave source regions are considered, but they may change into right-hand polarisation when propagating away from the source regions.

The group velocity of the wave is $\boldsymbol{V}_g = 2\pi F_c(H^+)\partial X/\partial \boldsymbol{k}$ where $\boldsymbol{k}$ is the wave vector and $F_c(H^+)$ is the proton cyclotron frequency. In this paper ψ is defined as the angle between $\boldsymbol{V}_g$ and $\boldsymbol{B}_E$, which indicates the group ray direction, and therefore

$$\boldsymbol{V}_g = V_{gz}\,\boldsymbol{e}_z + V_{g\perp}\boldsymbol{e}_\perp = V_g \cos\psi\,\boldsymbol{e}_z + V_g \sin\psi\,\boldsymbol{e}_\perp\,, \tag{3}$$

where $\boldsymbol{e}$ is the unit vector, and z and $\perp$ correspond to the directions parallel and perpendicular to $\boldsymbol{B}_E$ respectively. Here, the problem is treated as two-dimensional, and therefore $\boldsymbol{e}_\perp$ is in the plane containing $\boldsymbol{B}_E$ and $\boldsymbol{V}_g$. The method used here to calculate $\boldsymbol{V}_g$ was described by Leer *et al.* (1978).

The group velocities for the three wave classes are shown in Figs 2 and 3. In both figures, the top panels relate to $\theta = 10°$ and bottom panels to $\theta = 60°$. Fig. 2 shows the V_g–X relationship, and Fig. 3 gives the variation of the group ray angle ψ with X. In both figures, we used parameters $B_E = 300$ nT and $N(e) = 220\ \mathrm{cm}^{-3}$. This corresponds to the equatorial plasmapause region (e.g. $L \sim 4$–6). The intersection of the V_g curves for both left- and right-hand polarised modes at the crossover frequency confirms the existence of mode coupling at this frequency (see Fig. 2).

The relation between ψ and θ is an important feature for the propagation of waves. From Fig. 3, it is shown that class 1 has small ψ for all θ, and this

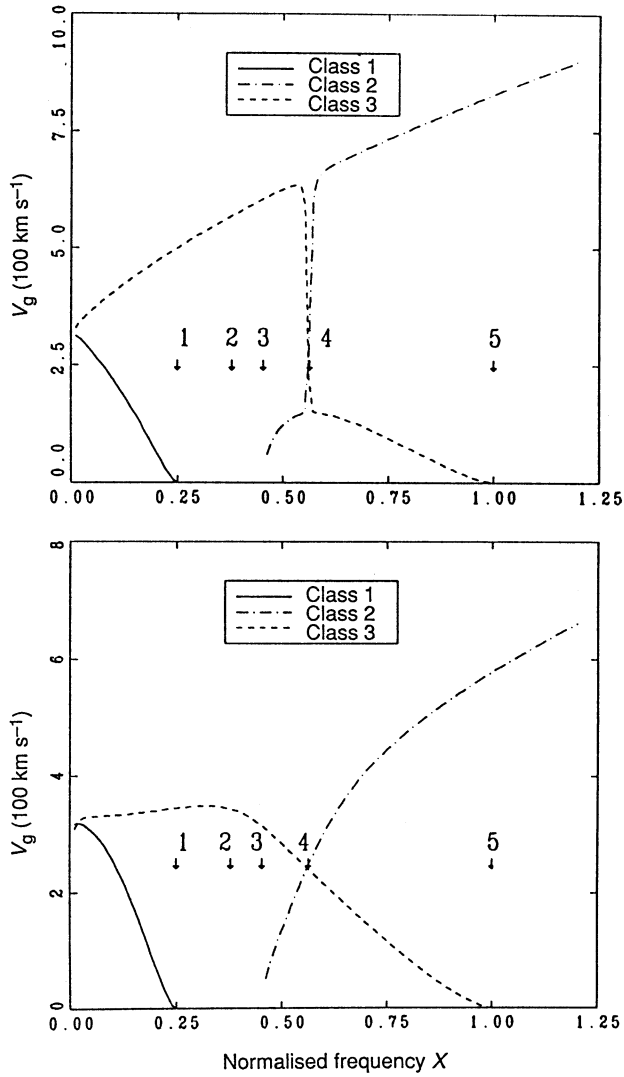

Fig. 2. Group velocity V_g in the same plasma as in Fig. 1. The top panel is for $\theta = 10°$ and the bottom for $\theta = 60°$. Arrows 1 to 5 indicate $X_c(He^+)$, X_{bi}, X_{cf}, X_{cr}, $X_c(H^+)$ respectively.

class of waves is described as guided waves. For class 2, ψ rapidly increases with increasing θ. This is a class of unguided waves. The higher frequency part of class 3 ($X > X_{bi}$) has a ψ–θ relationship similar to class 1, while the lower frequency part of class 3 ($X < X_{bi}$) shows unguided characteristics. For the waves of class 3, ψ is equal to zero at $X = X_{cr}$.

If θ is not close to 90°, classes 1 and 3 have ion cyclotron resonances at $X = X_c(He^+) = 0{\cdot}25$ and $X = X_c(H^+) = 1$ respectively, even though $\theta \neq 0$. However, if $\theta \to 90°$, the He^+ cyclotron resonance of class 1 disappears, and the H^+ cyclotron resonance of class 3 shifts to the bi-ion hybrid resonance. When θ

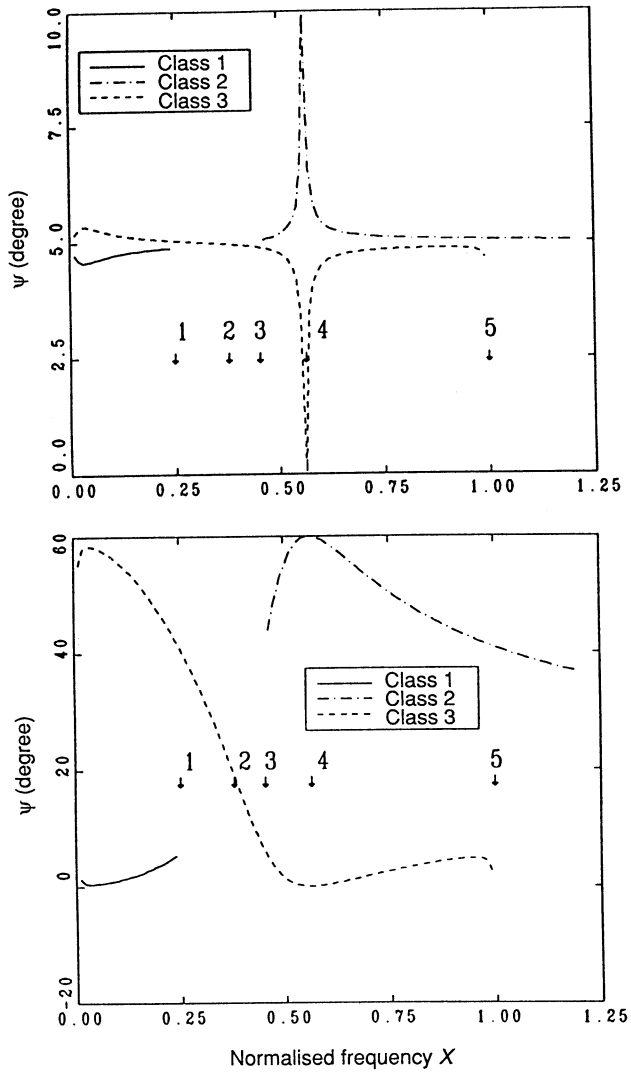

Fig. 3. Group ray angle ψ in the same plasma as in Fig. 1. The top panel shows $\theta = 10°$ and the bottom panel $\theta = 60°$. Arrows 1 to 5 indicate $X_c(He^+)$, X_{bi}, X_{cf}, X_{cr}, and $X_c(H^+)$ respectively.

is close to 90°, the waves become linearly polarised (not shown here, see Rauch and Roux 1982).

(2b) Oblique Wave Propagation in the Magnetosphere

In an inhomogeneous plasma, such as the magnetosphere, the characteristic frequencies vary in space. The features of wave propagation, therefore, will also change in space. Waves may be excited or amplified on and/or off the equatorial

region (Hu *et al.* 1990). Waves generated on the equator will propagate away from the equator, while waves generated in regions off the equator may propagate to higher latitude regions or back to the equator. The waves propagating from an off-equator source region to the equatorial region will experience a strong thermal damping (Hu *et al.* 1990). Therefore, these waves will be important for particle heating in the magnetosphere, but may contribute very little to the wave spectrum observed on the ground. Considering this, we calculate the wave travel time only for the waves propagating to higher latitude regions. In this case, the method used for both on- and off-equator sources will be the same. Therefore, in the following, we choose the plasma and wave parameters at the equator as the starting point. This relates to waves generated at the equator. For the waves produced by off-equator sources, the equatorial parameters should be replaced by the local parameters in the source regions.

When left-hand waves are generated by the ion cyclotron instability in the equatorial region of the magnetosphere, they may have frequencies as follows:

— equatorial class 1, i.e. $0 < X; < 0{\cdot}25$ at the equator;
— equatorial class 2 with $X_{\rm cf}(\mathrm{He}^+) < X < X_{\rm cr}(\mathrm{He}^+)$ at the equator;
— equatorial class 3 with $X_{\rm cr}(\mathrm{He}^+) < X < 1$ at the equator.

Hereafter, in the inhomogeneous magnetospheric plasma, the wave frequency and all characteristic frequencies will be normalised by the proton cyclotron frequency at the equator.

In order to investigate the propagation of waves in an inhomogeneous magnetosphere, models for both the geomagnetic field and the plasma density are required. In the present work, a centred dipole geomagnetic field model is used. The plasma density is modelled as $N = N_0\,P(r)$ with $P(r) = (r/r_0)^{-3}$, where N_0 is the density at the equator and $r = r_0\cos^2\lambda$, with $r_0 = LR_{\rm E}$, $R_{\rm E}$ the Earth's radius and λ the latitude. It is also assumed that $N(\mathrm{He}^+)/N(\mathrm{e})$ remains constant ($0{\cdot}27$) along the wave path. We consider waves produced near the plasmapause ($L \sim 4$–6). In the equatorial region, $B_{\rm E}$ is taken to be 300 nT. The cold electron density at the equator is assumed to be 220 cm^{-3}. Hereafter, the wave frequency X and characteristic frequencies (e.g. $X_{\rm c}$, $X_{\rm cr}$, $X_{\rm cf}$ and $X_{\rm bi}$) at a spatial location in the magnetosphere are normalised to the equatorial proton cyclotron frequency of the same field line.

Fig. 4 shows the variation of $X_{\rm c}(\mathrm{H}^+)$, $X_{\rm cr}$, $X_{\rm cf}$, $X_{\rm bi}$ and $X_{\rm c}$ (He^+) along a magnetic field line in the magnetosphere. During wave propagation, X remains constant in this figure while the characteristic frequencies increase with geomagnetic latitude. The waves of class 1 always have $X < X_{\rm c}(\mathrm{He}^+)$ when propagating in the magnetosphere. The waves of class 2 may reach a cutoff point where $X = X_{\rm cf}$. The waves of class 3 may first reach a crossover point where $X = X_{\rm cr}$, and then arrive at a hybrid resonant point where $X = X_{\rm bi}$. Because the polarisation of the waves of class 3 has reversed after the waves pass the crossover point, both the cutoff point where $X = X_{\rm cf}$ and the point where $X = X_{\rm c}(\mathrm{He}^+)$ do not affect the propagation.

The variation of θ in the magnetosphere is important since this controls the dispersion characteristics. The position of wave reflection and the wave path are also controlled by θ. The value of θ initially depends on the mechanism which destabilises the waves. Dobes (1970), Oscarsson and Andre (1986) and Ludlow (1989) showed that the ion cyclotron instability has large growth rates distributed

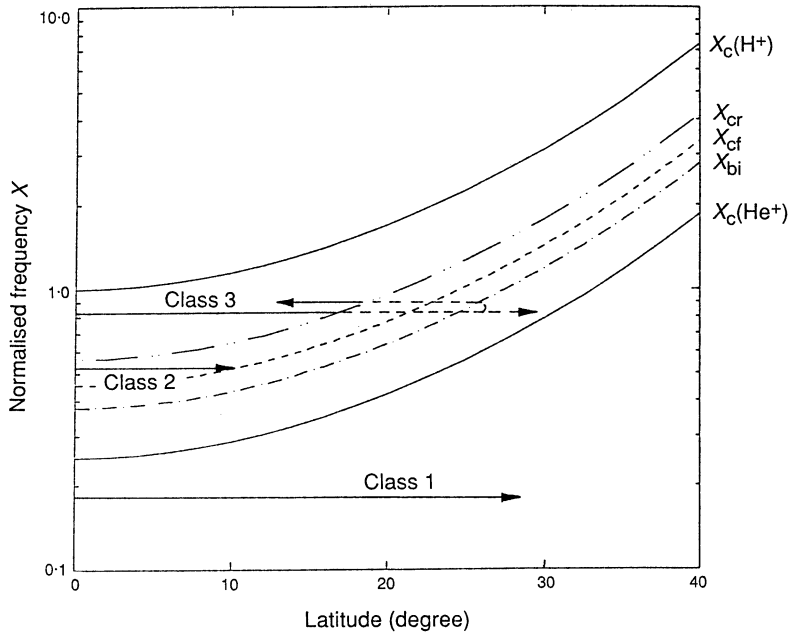

Fig. 4. Variation of the characteristic frequencies with latitude in the magnetosphere. Three wave branches are also shown. For the class 3 wave, the solid part of the line indicates the left-hand polarisation and the dashed part shows right-hand polarisation.

from $\theta = 0$ to $\sim 30°$, and there may be another peak at $\theta \sim 70°$. This provides a measure of θ in the wave source regions. In order to determine the variation of θ when the waves propagate in the magnetosphere, we assume that ray propagation can be used for the waves under consideration. This ray approach is valid if the spatial and temporal variations of the plasma are slow when compared with the wavelength and frequency, according to WKB theory (e.g. Born and Wolf 1959; Yeh and Liu 1972). Here, we consider only the spatial variation of the plasma. In Section 3, we will compare the typical length of wave path in the magnetosphere and the wavelength, and examine the validity of the ray approach. Strictly, the ray propagation of the waves should be investigated by solving the ray equations in an inhomogeneous plasma (Haselgrove 1955; Kelso 1964; Stavroudis 1972). However, we will use a simplified method with some additional assumptions.

It is known (e.g. Kelso 1964) that the differential equation for ray propagation is equivalent to a generalised form of Snell's law:

$$\frac{\mathrm{d}}{\mathrm{d}t}\left(n\frac{\boldsymbol{\sigma}}{|\boldsymbol{\sigma}|}\right) = c\,|\boldsymbol{\sigma}|^{-1}\nabla n, \tag{4}$$

where $\boldsymbol{\sigma}$ is a vector defined by $\boldsymbol{\sigma} = n\boldsymbol{k}/|\boldsymbol{k}|$ with $\boldsymbol{k}$ being the wave vector. The index n varies in the inhomogeneous plasma, and therefore $\boldsymbol{\sigma}$ varies spatially.

When the wave propagates, both n and $\boldsymbol{\sigma}$ vary, and so equation (4) describes the variation of $\boldsymbol{k}$ during propagation. We are interested in the wave propagation along geomagnetic field lines, namely the guided or quasi-guided propagation, which is thought to be the basic propagation pattern for the waves which may be recorded on the ground (e.g. Roux *et al.* 1982; Rauch and Roux 1982; Fraser 1985). Equation (4) should generally be treated as a three-dimensional problem. In order to obtain the variation of $\boldsymbol{\sigma}$ (or $\boldsymbol{k}$), equation (4) must be integrated along the wave path. If the wave path is known it may be assumed that the inhomogeneous plasma is approximately stratified along the wave path, and thus the problem may be simplified to become one-dimensional. Because full ray tracing has already shown that the paths for waves which may reach the ground are mainly along field lines, ∇n may be assumed also to be field-aligned. In this case, equation (4) gives $\mathrm{d}(n\sin\theta)/\mathrm{d}t = 0$ in the plane perpendicular to ∇n. Therefore, the wave normal angle at any point along field lines is given by

$$n(\theta, \lambda)\sin\theta = n(\theta_0, \lambda_0)\sin\theta_0\,, \tag{5}$$

where λ is the geomagnetic latitude, and subscript 0 refers to the initial value at the equator. We will use equation (5) to study the variation of θ along a field line. Angle ψ can also be obtained along the field line from θ. We should mention that the method for calculating θ along a wave path has been used in other studies of Pc 1–2 waves (e.g. Dowden 1965). Because Snell's law, i.e. equation (5), is based on the approximation that ∇n is field-aligned, the validity of the results from equation (5) will also be discussed for each class of wave.

Class 1 ($X < 0{\cdot}25$). Variations of θ and ψ for class 1 waves with λ are plotted in Fig. 5. The basic characteristics of these waves are the same as those discussed by Dowden (1965), where we replace H^+ with He^+ because H^+ rarely affects the He^+ cyclotron waves. The figure shows that θ is almost 90° when the waves reach the bottom of the magnetosphere (latitude ~62·5°). This result also agrees well with that obtained from ray tracing studies (Kitamura and Jacobs 1968; Rauch and Roux 1982). Because the waves are guided ($\psi < 12°$ always), the assumption of field-aligned propagation is valid.

Class 2 ($0{\cdot}453 < X < 0{\cdot}564$). In Fig. 6 the variation of θ and ψ for class 2 waves is shown for $\theta_0 = 10°$, 30° and 60° and $X = 0{\cdot}48$ and $0{\cdot}53$. This figure shows that θ and ψ remain roughly constant near their initial values (θ_0 and ψ_0) before the waves propagate to regions where the wave frequencies match the local cutoff frequency. Where $X \sim X_{\mathrm{cf}}$, θ and ψ increase rapidly to 90°, and the waves may be reflected. Rauch and Roux (1982) reported that the reflected waves propagate outwards to lower geomagnetic field regions.

The curves corresponding to the $\theta_0 = 60°$ case indicate that caution should be observed when dealing with large θ_0, because in this situation ψ is large, and therefore the assumption that the wave group ray travels along the field line may become invalid. However, even for $\theta_0 \sim 0$–30°, the ray is still reasonably close to the field line before reaching the cutoff point.

Class 3 ($0{\cdot}546 < X < 1$). Fig. 7 shows the variation of θ and ψ as a function of latitude for class 3 waves of different θ_0 and X ($0{\cdot}564 < X < 1$). It

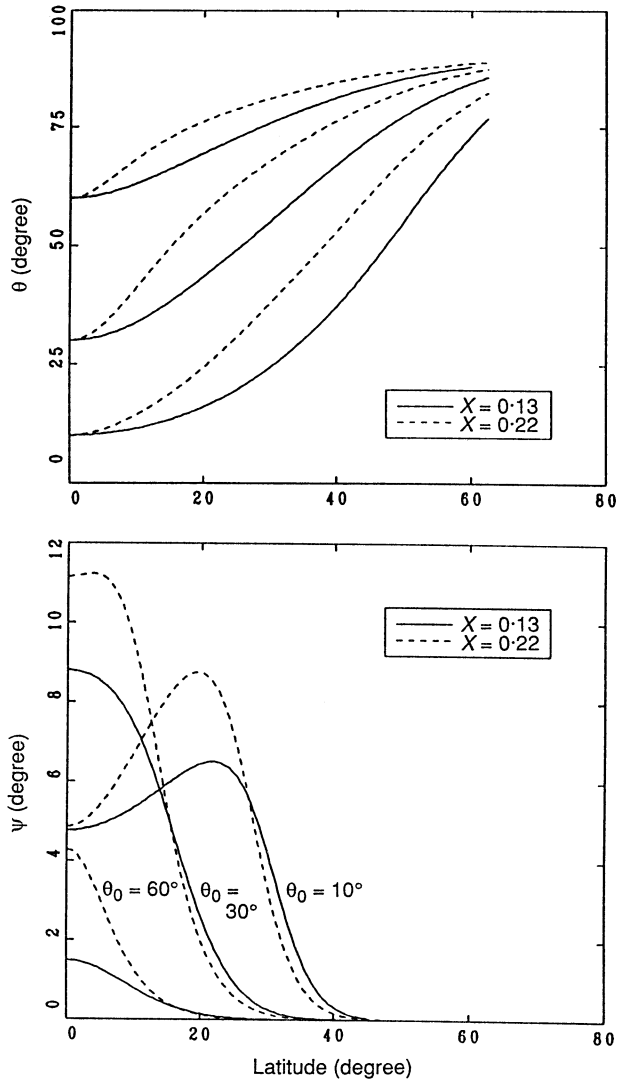

Fig. 5. Variation of θ (top panel) and ψ (bottom panel) with latitude for class 1 waves, along the $L = 4{\cdot}7$ field line. Equatorial wave normal angles θ_0 are 10°, 30° and 60°.

can be seen that at the point where $X = X_{cr}$, ψ is equal to zero, agreeing with the result that $\psi = 0$ when $X = X_{cr}$ as described before (see Fig. 3).

The upper panel of Fig. 7 shows that, when θ_0 is small, θ increases slowly with λ until λ reaches a large value, while in the lower panel ψ remains small until θ starts to increase rapidly. For example, when $\theta_0 = 10°$ and $X = 0{\cdot}61$, ψ remains small (<20°) until $\lambda \sim 40°$. When λ is as large as ~52°, θ and ψ will increase rapidly to 90°. Thus, the smaller θ_0 and the lower X, the farther the waves propagate along field lines.

Although we are unable to use the point where both θ and ψ are equal to 90° to define exactly where the waves are reflected, it is possible to use this point

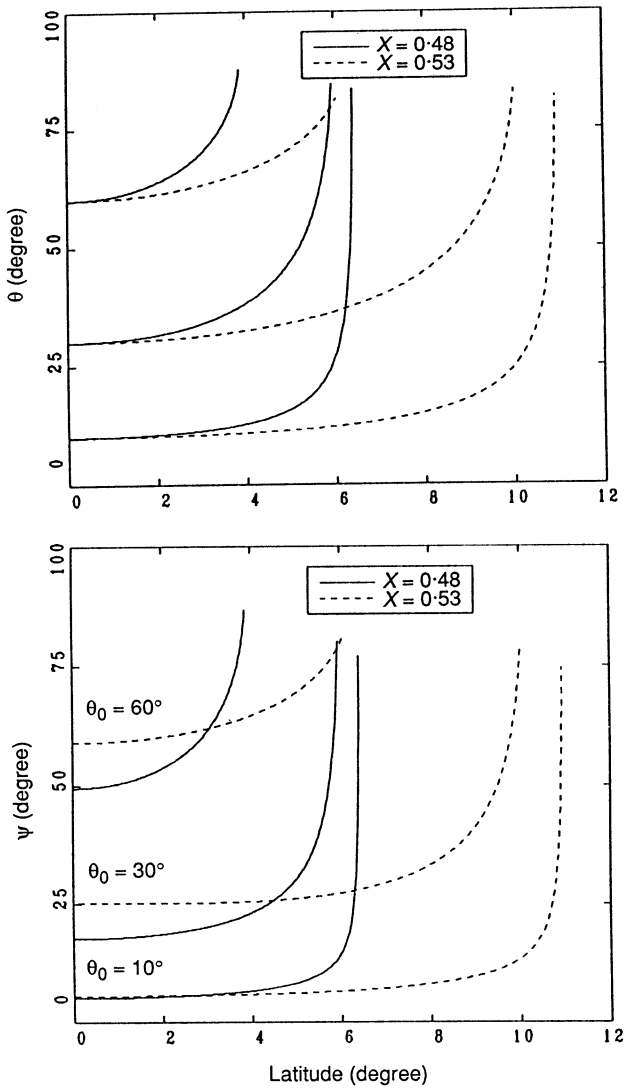

Fig. 6. Similar to Fig. 5, but for class 2 waves.

to roughly estimate the reflection region. This follows from the rapid increase in ψ with λ near the reflection region; thus the point at which both θ and ψ are equal to 90° probably does not deviate far from the reflection point. Fig. 8 shows the latitude where $\theta = \psi = 90°$ for various X and θ_0. It can be seen that, if θ_0 is large (e.g. the $\theta_0 = 60°$ case in Fig. 8) or X is close to 1, θ becomes 90° near and often above the point at which $X = X_{\mathrm{bi}}$. This indicates that the reflection takes place near the point at which $X = X_{\mathrm{bi}}$ (e.g. Rauch and Roux 1982). However, when θ_0 is small and X is close to X_{cr}, the reflection point may be located at latitudes higher than that determined by $X = X_{\mathrm{bi}}$. In our view, wave reflection is due to $\theta = \psi = 90°$ which is determined by Snell's law and the wave dispersion relation, and therefore the reflection point depends

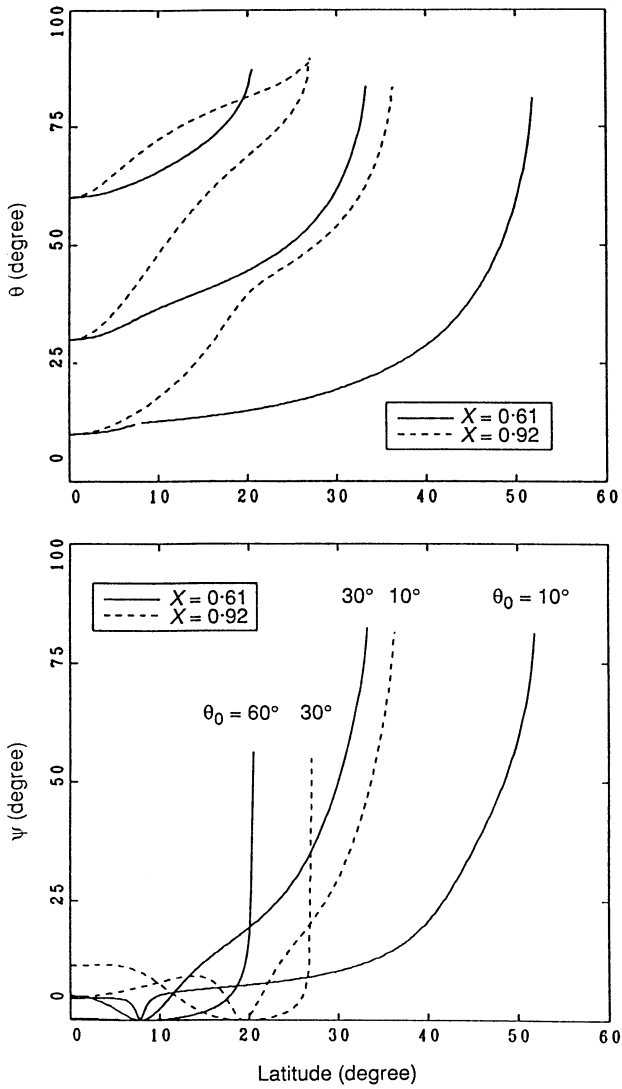

Fig. 7. Similar to Fig. 5, but for class 3 waves.

on θ_0 and X. This result differs from that of Rauch and Roux (1982), which showed that the reflection was always in the bi-ion hybrid resonance region where $X = X_{bi}$, and independent of X and θ_0.

It is necessary to mention that the higher reflection latitude for smaller θ_0 and X is not considered to be introduced by the approach used in our method. Because both θ and ψ are small over a wide range of latitudes (see the $X = 0{\cdot}61$ and $\theta_0 = 10°$ curve in Fig. 7), the assumption that the waves propagate along the field line is valid, and therefore the result should be reliable.

(2c) Wave Group Travel Time

With the above preparation, we can now estimate the group travel time for waves propagating in the magnetosphere from the equator to the reflection points.

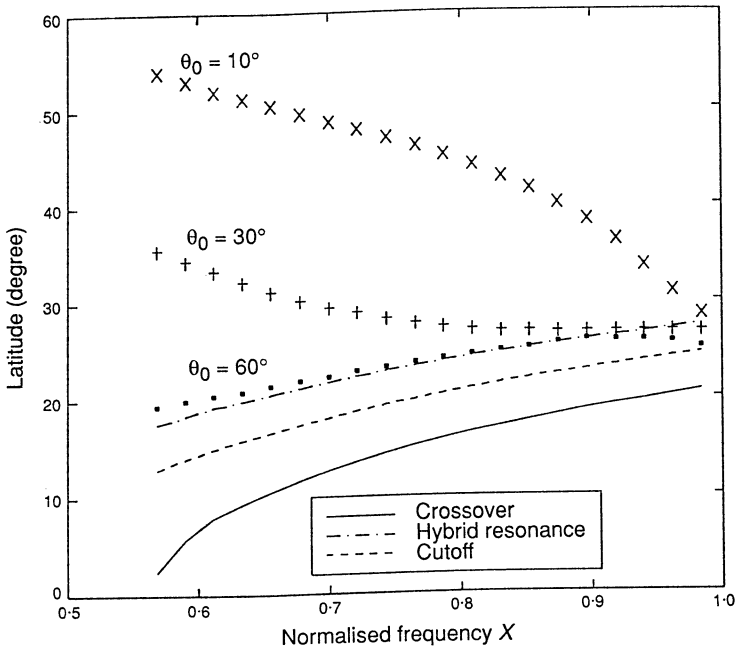

Fig. 8. Positions where $\theta = \psi = 90°$ for the waves of class 3 with various θ_0 (10°, 30° and 60°). The curves indicate the regions where $X = X_{cr}$ (crossover), $X = X_{bi}$ (hybrid resonance) and $X = X_{cf}$ (cutoff) are located.

We still assume that the wave ray path is along a field line, so that the results obtained in the above calculations can be used. This one-dimensional treatment should be reasonable for most waves which can reach the ground (e.g. classes 1 and 3). The group travel time T_g is written as

$$T_g = \int_0^{\lambda_0} (V_g \cos\psi)^{-1} \, ds \,, \tag{6}$$

where λ_0 is the latitude at which both θ and ψ are equal to 90°, i.e. the reflection point. The integration is performed along the field line, and therefore $ds = LR_E \cos\lambda \, (4-3\cos^2\lambda)^{1/2} \, d\lambda$. For class 1 and 3 waves, the wave bounces between the two hemispheres with a bounce period of $T = 4T_g$. In equation (6), λ_0, V_g and ψ depend on X and θ_0 and have been given in the subsection above.

Using parameters along the $L = 4{\cdot}7$ field line, we have $\lambda_0 \approx 62{\cdot}5°$ for class 1 waves, and λ_0 for class 3 waves is the latitude at which $\theta = \psi = 90°$, as discussed in Section *2b* (shown in Fig. 8). For class 2, the waves are unguided, and therefore only the integration results with small θ_0 may be used to estimate the travel time from the wave source region to the reflecting point.

Fig. 9 displays the results of the integral T_g normalised by

$$T_a = \int_0^{62{\cdot}5^\circ} V_a^{-1} \, ds \,, \tag{7}$$

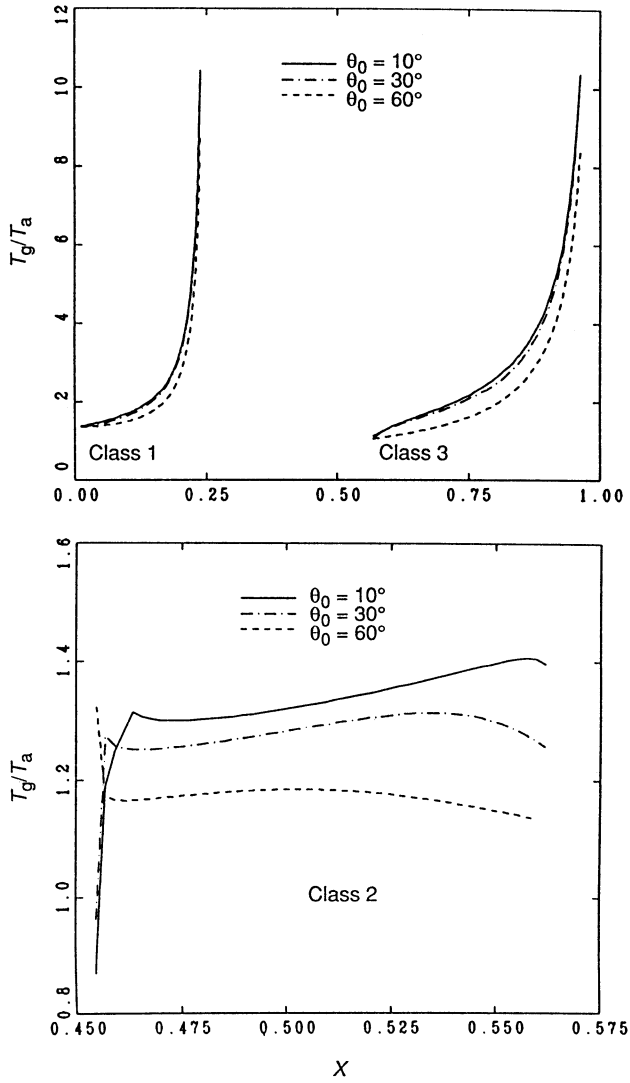

Fig. 9. Group travel time for waves propagating from the equator to the point where $\theta = 90°$. The top panel shows classes 1 and 3, and the bottom class 2 waves.

where $V_a = |\boldsymbol{B}_E|/[4\pi N(e)\, m(H^+)]^{1/2}$ is the local Alfvén velocity in a proton plasma. The top panel relates to classes 1 and 3. For the class 1 waves, an increase in θ_0 decreases T_g. The important property for this wave class is that the spectral tone (i.e. X–T_g relationship) still shows increasing slope, the same as Pc 1–2 waves in the e^-–H^+ plasma case (e.g. Dowden 1965). For class 3 waves, the spectral tone and T_g–θ_0 relationships are similar to those of class 1, and the tone is also rising. Since V_a in equation (7) is the Alfvén velocity for a proton plasma with the same electron density as that used in our two-ion plasma model, the Alfvén velocity in the two-ion plasma is

$$V_a\{N(e)m(H^+)/[m(He^+)N(He^+) + m(H^+)N(H^+)]\}^{1/2}.$$

Therefore, the quantity

$$T_a\{[m(He^+)N(He^+) + m(H^+)N(H^+)]/m(H^+)N(e)\}^{1/2} \approx 1{\cdot}4T_a$$

is the group travel time for Alfvén waves from the equator to the ground. In Fig. 9, it is seen that when $X \to 0$, $T_g/T_a \to 1{\cdot}4$ for class 1 because the wave tends to an Alfvén wave. When X tends to the normalised crossover frequency for class 3, T_g/T_a tends to a value between $1{\cdot}2$ and $1{\cdot}4$. This indicates that class 3 waves, which may be reflected at low latitudes, show group travel times comparable with those of waves that are reflected at the ionosphere. This is a consequence of the property that the greatest contribution to the group travel time occurs in the equatorial region where V_g is a minimum.

The bottom panel of Fig. 9 shows the group travel time for class 2 waves. Since the class 2 waves may propagate at large ψ when θ is large, only the curves with small θ_0 roughly indicate the group travel time to the location where the wave may be reflected to the outer magnetosphere. From the curves for $\theta_0 = 10°$ and 30° it can be seen that the variation of T_g is not large for class 2 waves. When X is not close to X_{cf} at the equator, T_g/T_a values range between $1{\cdot}2$ and $1{\cdot}4$. Because there is no bounce between the hemispheres for class 2 waves, T_g does not relate to a bounce period.

An important feature of the X–T_g relationship is that both classes 1 and 3 waves exhibit dispersion which corresponds to rising tones. If only waves of class 1 or class 3 are generated in the source region, we may observe a rising tone on the ground. If both classes 1 and 3 are generated simultaneously, it is possible for the predicted wave spectra to display two bands, both of which exhibit rising tones. This result indicates that the wave propagation from low to high latitudes in a multi-component magnetosphere cannot support a falling tone in the wave spectrum, provided that the mode coupling is included. This will be discussed in the next section.

3. Discussion

(3a) Ray Approximation and One-dimensional Model

Ray propagation for the waves has been used to calculate the variation of θ along a field line. This implies the assumption that in the region of interest the relevant dimensions of the wave paths are much larger than the wavelength of the propagating waves. In order to confirm this assumption, Fig. 10 shows the variation of the wavelength for typical waves in class 1 ($X = 0{\cdot}219$), class 2 ($X = 0{\cdot}503$) and class 3 ($X = 0{\cdot}656$) at $L = 4{\cdot}7$. Normally, the wavelength L_w is less than 500 km if the position is not close to the reflection points. Using L_d to express the length of the wave path from $\lambda = 0$ to λ_0 along the field line, it can be shown that $L_w/L_d \lesssim 0{\cdot}005$ for class 1 and $L_w/L_d \lesssim 0{\cdot}02$ for class 3. The typical wavelength of class 2 is about 300 km if the latitude is not near the cutoff point, but the wavepath is shorter than those of classes 1 and 3. In this case, if X is not near X_{cf} at the equator, $L_w/L_d \sim 0{\cdot}05$–$0{\cdot}1$. Therefore, the ray approach appears justified for most of the frequencies and regions we have considered.

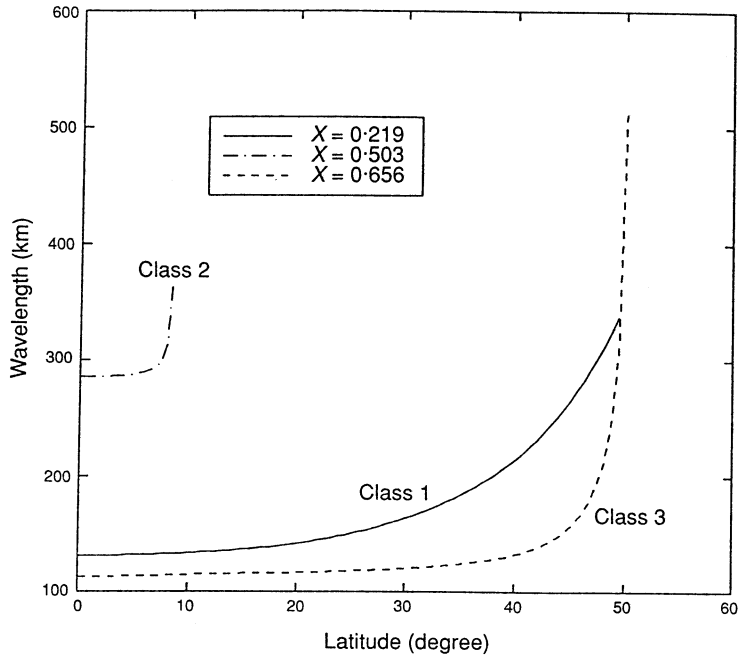

Fig. 10. Variation of wavelength in the magnetosphere for typical waves of class 1 ($X = 0{\cdot}219$), class 2 ($X = 0{\cdot}503$) and class 3 ($X = 0{\cdot}656$). The wave normal angle at the equator is $\theta_0 = 10°$.

In the following regions the ray approximation is invalid because L_w/L_d is too large:

— the region where $X \sim X_{cf}$ (class 2, this is of little interest);

— the region where $X \sim X_{bi}$ (class 3).

Perraut *et al.* (1984) showed that the region where $X \sim X_{bi}$ reflects a fraction of the wave energy, and allows the remainder to be transmitted. The transmission process also acts as a lowpass filter. Although the ray approach is invalid in the region where $X \sim X_{bi}$ and Snell's law may also be invalid because ψ becomes large in this region, these restrictions do not lead to significant errors in the calculation of T_g. This is because most of the ray travel time is accumulated in the lower latitude and equatorial regions.

To simplify the problem we have used Snell's law to investigate the variations of both θ and ψ along a wave path which is assumed to be field-aligned. This treatment is based on the fact that we already know that the wave paths of the waves of classes 1 and 3, which can reach the ground, are almost parallel to the field line. For a known wave path, the assumption that ∇n is parallel to the tangential direction of the wave path is reasonable. Thus equation (4) is acceptable for our one-dimensional treatment. However, if the ray deviates too far from the field line, two- or three-dimensional ray tracing must be considered. Our calculation confirms that, for class 1 waves, the one-dimensional method is applicable because the waves are guided (i.e. ψ is always small), and for class

3 waves, the method is also considered suitable because ψ is small in most propagation regions. For class 2 waves, if θ is initially small, then ψ does not become large until the waves reach the point where $X \sim X_{cf}$.

Finally, we note that the one-dimensional treatment used here provides a simple method to evaluate propagation path latitudes and plasma densities in a multi-ion plasma. This method was widely used in the e^-–H^+ plasma (e.g. Dowden and Emery 1965; Fraser 1968).

(3b) Can a Wave Spectral Tone be Changed by Wave Propagation Effects?

Considering only the parallel propagation of left-hand polarised waves, Dowden (1966) suggested that a 'nose' type ('<' type) frequency–time structure seen in dynamic spectra for Pc 1–2 waves recorded on the ground was due to a propagation effect for wave normalised frequencies in the region $X_{cf} < X < 1$ at the equator. However, this theory was based on two assumptions:

(i) the waves remained left-hand polarised during propagation; and
(ii) the heavy ions were present only near the equator.

The first assumption implies that wave propagation is strictly parallel to $\boldsymbol{B}_E$, and the second is only applicable when the concentration of heavy ions is as low as $\sim 0{\cdot}001$ off the equator (see the following discussion). Hence, these approximations do not describe a realistic magnetosphere.

Considering the minimum in V_g for right-hand polarised waves with $X_{bi} < X < X_{cr}$ (see Fig. 2), Gendrin and Laurent (1979) suggested that a wave propagation effect may be one of the factors which leads to a wave spectral tone in the form of a Chevron type ('>' type). But, this consideration requires that the waves remain right-hand polarised during propagation, a situation which is also unacceptable.

By careful examination of the parameters involved in altering the spectral tone through a wave propagation effect, we find that V_g must exhibit a maximum in the equatorial region at the frequency at which spectral tone changes from rising to falling. This is because most of the group travel time is spent in this region, so the maximum V_g normally corresponds to the earliest arrival of the wave packet, while waves at higher and lower frequencies will reach the observer later, forming a nose tone ('<' type). Similarly, if the senses of all the extrema are reversed, a chevron spectral tone ('>' type) results. Therefore, the change in the spectral tone occurs only when the V_g–X curve exhibits a V_g maximum (for '<' type) or a minimum (for '>' type) at a certain X. Now, consider the propagation of EM waves with frequencies near the ion cyclotron frequencies. In general, there are five possible cases:

Case 1: Parallel propagation of left-hand polarised waves.—In this case, V_g has a maximum near X_{cr}, so a '<' type spectrum may be formed for the waves which are mixed from the left-hand fractions of classes 2 and 3. However these waves can hardly contribute to ground observations because they cannot pass the stop region for left-hand polarised waves, since the region where $X \sim X_{cf}$ can reflect the left-hand polarised waves. A consideration of wave attenuation in the stop region will also confirm that left-hand wave transmission through the stop band in the magnetosphere is impossible. Dowden (1966) showed that an amplitude decrease across the stop region was only 2–3 dB. However, this result was based on an assumption that $N(H^+)/N(He^+) \sim 1000$ (very low heavy ion

concentration). In fact, the heavy ion concentration in the magnetosphere is much higher than this value. If we take a typical measured value of $N(H^+)/N(He^+) \lesssim 10$ (see Section 2) and use the same method as that used by Dowden (1966), it can be shown that the wave amplitude decrease is $\gtrsim$150 dB. This decrease is much larger than the total amplification of the waves through the ion cyclotron instability (~10–50 dB, see Hu *et al.* 1990). Thus, this result indicates that the left-hand waves are unlikely to pass through the stop region.

Case 2: Parallel propagation of right-hand polarised waves.—V_g does not have a minimum or a maximum, and the spectral tone is always falling. Furthermore, these waves cannot be normally generated by the ion cyclotron instabilities.

Case 3: Oblique propagation of left-hand polarised waves.—This wave propagation pattern corresponds to the waves mixed by the left-hand polarised fraction of classes 2 and 3. Similar to the parallel propagation of left-hand waves, a '<' type nose effect appears to result because of the maximum in V_g near X_{cf}. However, this case cannot exist when mode coupling occurs. From the bottom panel of Fig. 1, it is seen that when θ is large the mixing of left-hand branches of the class 2 and 3 waves is impossible.

Case 4: Oblique propagation of right-hand polarised waves.—In this case, V_g has a minimum between $X \sim X_{bi}$ and $X \sim X_{cr}$, so a '>' type spectrum could be formed (note that the minimum in V_g does not occur when $\theta = 0$). This wave propagation pattern is associated with the waves mixed by the right-hand polarised fractions of classes 2 and 3. However, this pattern can hardly exist in the magnetosphere, because

(i) mode coupling occurs (because propagation is oblique) so that the waves cannot remain right-hand polarised when they propagate to the region where $X \sim X_{cr}$; and

(ii) the waves with frequency below the proton frequency are normally generated with left-hand polarisation.

Case 5: Oblique propagation of coupled waves—Since mode coupling occurs, the spectra always display rising tones.

Fraser (1972) found that only those nose emissions ('<' type) with X close to X_{cf} might agree with Dowden's theory, and the associated concentration of He^+ was low (~0·001–0·01). He pointed out that for the nose emissions with higher frequency, the explanation using the propagation effect in an e^-–He^+–H^+ plasma was invalid. This supported the idea that the Dowden theory for the parallel propagation of left-hand waves may be applicable only for low heavy ion concentrations.

From this analysis, we have seen that the most probable propagation mechanism leading to ground wave observation above $X_c(He^+)$ is the oblique propagation of coupled waves. If the concentration of heavy ions is very low (~0·001–0·01), the nose effect suggested by Dowden may occur and provide ground observations. However, the heavy ion concentrations observed by satellites in the magnetosphere are much higher (~0·1–0·5) than that allowed by Dowden's theory. Therefore, the ground recorded waves are most likely to propagate obliquely and, as the discussion has indicated, the nose and Chevron effects (both '<' and '>' types) cannot be produced by the propagation of waves in a multi-ion plasma.

Fraser (1972) mentioned that the observation of nose emissions does not necessarily indicate propagation in a multi-ion medium. It was suggested that

the propagation of two or more adjacent narrow-band emissions along slightly different field lines might be considered as an alternative explanation for the nose effect. In addition to this, the following factors may also contribute to the formation of the nose or Chevron spectral forms:

(i) a change of slope of the X–t spectrum by an ion cyclotron instability (e.g. Gendrin *et al.* 1971; Gendrin and Laurent 1979);
(ii) nonlinear dispersion effects for the waves with large amplitudes. For example, a large amplitude wave packet may be described by a nonlinear Schrödinger equation (e.g. Hasegawa 1975) which contains a contribution from nonlinear dispersion.

(3c) Other Issues

The phenomenon of Pc 1–2 wave packets bouncing between conjugate reflection locations allows sufficient time for wave amplification through a resonant interaction with energetic ions in the ring current. However, the explanation of the mirroring effect for the different wave branches is different. For class 1, the reflection occurs at the top of the ionosphere. From the variation of θ with λ, we have seen that near this region $\theta \sim 90°$. For class 3, location of the reflection region depends on the wave frequency, initial θ, and plasma parameters such as the concentration of heavy ions. In our model, the latitude of the reflecting point can be roughly estimated by the point at which $\theta = \psi = 90°$ (Fig. 8).

We should point out that after several bounces θ_0 may increase for class 3 waves (Rauch and Roux 1982). Therefore, the bounce period may also be affected by the number of bounces. However, since a significant fraction of the wave energy of class 3 passes through the reflection region (Perraut *et al.* 1984), the reflected waves must be amplified so that they can maintain sufficient energy to sustain the bouncing wave packet. The ion cyclotron instability which allows wave amplification is confined to small θ_0 ($<30°$) or $\theta_0 \sim 60°$ (see Section 2). This may offset the propagation effect that θ_0 increases with successive bounces.

4. Conclusions

We have developed a method to calculate the dispersion spectra of waves that have frequencies near the ion cyclotron frequencies, and which propagate obliquely in the magnetosphere. Mode coupling between the left- and right-hand waves is included. This leads to a significant modification of the frequency–group travel time relationship. The method provides the potential for estimating the plasma parameters in a multi-component magnetosphere using Pc 1–2 X–t spectra. Other important results obtained include:

— Only a rising tone in the X–t spectrum can be formed by the wave propagation effects associated with classes 1 and 3 when mode coupling is included. Class 2 cannot reach the ground, and is of no importance.

— The reflection latitude of the class 3 waves is determined by θ_0 and X, and may extend to higher latitudes along the field line when both θ_0 and X are small.

Acknowledgments

This work was supported by the University of Newcastle and the Australian Research Council. We acknowledge Dr H. Hansen for helpful discussions.

References

Balsiger, H., Geiss, J., and Young, D. T. (1983). *In* 'Energetic Ion Compositions in the Earth's Magnetosphere' (Ed. R. G. Johnson), p. 195 (Terra Scientific: Tokyo).

Born, M., and Wolf, E. (1959). 'Principles of Optics' (Pergamon: New York).

Chen, L. (1987). 'Waves and Instabilities in Plasmas' (World Scientific: Singapore).

Dobes, K. (1970). *Planet. Space Sci.* **18**, 395.

Dowden, R. L. (1965). *Planet. Space Sci.* **13**, 761.

Dowden, R. L. (1966). *Planet. Space Sci.* **14**, 1273.

Dowden, R. L., and Emery, M. W. (1965). *Planet. Space Sci.* **13**, 773.

Fraser, B. J. (1968). *Planet. Space Sci.* **16**, 111.

Fraser, B. J. (1972). *Planet. Space Sci.* **20**, 1883.

Fraser, B. J. (1982). *Planet. Space Sci.* **30**, 1299.

Fraser, B. J. (1985). *Space. Sci. Rev.* **42**, 357.

Fraser, B. J., and McPherron, R. L. (1982). *J. Geophys. Res.* **87**, 4560.

Fraser-Smith, A. C. (1977). *Geophys. Res. Lett.* **4**, 53.

Geiss, J., Balsiger, H., Eberhardt, P., Walker, H.-P., Weber, L., Young, D. T., and Rosenbauer, H. (1978). *Space Sci. Rev.* **22**, 537.

Gendrin, R., Lacourly, S., Roux, A., Solomon, J., Feygin, F. Z., Gokhberg, M. V., Troitskaya, V. A., and Yakimenko, V. L. (1971). *Planet. Space Sci.* **19**, 165.

Gendrin, R., and Laurent, G. (1979). *Geophys. Res. Lett.* **6**, 197.

Gurnett, D. A., Shawhan, S. D., Brice, N. M., and Smith, R. L. (1965). *J. Geophys. Res.* **70**, 1665.

Hasegawa, A. (1975). 'Plasma Instability and Nonlinear Effects' (Springer: Berlin).

Haselgrove, J. (1955). *In* 'The Physcis of the Ionosphere', pp. 355 (The Physical Society: London).

Higuchi, Y. (1985). *J. Geomag. Geoelect.* **37**, 999.

Higuchi, Y., and Jacobs, J. A. (1970). *J. Geophys. Res.* **75**, 7105.

Higuchi, Y., Kisabeth, J. L., and Jacobs, J. A. (1972). *Planet. Space Sci.* **20**, 707.

Hu, Y. D. (1991). Electromagnetic waves in the magnetosphere with frequencies near the ion cyclotron frequency: propagation, amplification and wave–particle interaction. Ph.D. thesis, Univ. Newcastle, N.S.W.

Hu, Y. D., Fraser, B. J., and Olson, J. V. (1990). *Geophys. Res. Lett.* **17**, 1053.

Inhester, B., Wedeken, U., Korth, A., Perraut, S., and Stockholm, M. (1984). *J. Geophys.* **55**, 134.

Jacobs, J. A., and Watanabe, T. (1964). *J. Atmos. Terr. Phys.* **26**, 825,

Kelso, J. M. (1964). 'Radio Ray Propagation in the Ionosphere' (McGraw–Hill: New York).

Kitamura, T., and Jacobs, J. A. (1968). *Planet. Space Sci.* **16**, 863.

Leer, E., Johansen, K. M., and Albrigtsen, R. (1978). *J. Geophys. Res.* **83**, 3125.

Ludlow, G. R. (1989). *J. Geophys. Res.* **94**, 15385.

Mauk, B. H., McIlwain, C. E., and McPherron, R. L. (1981). *Geophys. Res. Lett.* **8**, 103.

Obayashi, T. (1965). *J. Geophys. Res.* **70**, 1069.

Oscarsson, T., and Andre, M. (1986). *Ann. Geophysicae* A **4**, 319.

Perraut, S., Gendrin, R., Roux, A., and de Villedary, C. (1984). *J. Geophys. Res.* **89**, 195.

Rauch, J. L., and Roux, A. (1982). *J. Geophys. Res.* **87**, 8191.

Roux, A., Perraut, S., de Villedary, C., Gendrin, R., Kremser, G., Korth, A., and Young, D. T. (1982). *J. Geophys. Res.* **87**, 8174.

Smith, R. L., and Brice, N. M. (1964). *J. Geophys. Res.* **69**, 5029.

Stavroudis, O. N. (1972). 'The Optics of Rays, Wavefronts, and Caustics' (Academic: New York).

Stix, T. H. (1962). 'The Theory of Plasma Waves' (McGraw–Hill: New York).

Tepley, L. R. (1966). *J. Geomag. Geoelect.* **18**, 227.

Yeh, K. C., and Liu, C. H. (1972). 'Theory of Ionospheric Waves' (Academic: New York).

Young, D. T., Perraut, S., Roux, A., de Villedary, C., Gendrin, R., Korth, A., Kremser, G., and Jones, D. (1981). *J. Geophys. Res.* **86**, 6755.

Manuscript received 7 May, accepted 14 July 1992